Cryo-EM structure of a single-chain β1-adrenoceptor – AmpC β-lactamase fusion protein

Gabriella Collu[1,2], Inayathulla Mohammed[3], Aleix Lafita[4], Tobias Bierig[1,2], Emiliya Poghosyan[1], Spencer Bliven[5], and Roger M. Benoit[1*]

[1]Laboratory of Nanoscale Biology, Division of Biology and Chemistry, Paul Scherrer Institute, CH-5232 Villigen PSI, Switzerland

[2]Department of Biology, ETH Zürich, 8093 Zürich, Switzerland

[3]BioEM, Biozentrum, University of Basel, Basel, Switzerland

[4]Laboratory of Biomolecular Research, Division of Biology and Chemistry, Paul Scherrer Institute, CH-5232 Villigen PSI, Switzerland

[5]Science IT Infrastructure and Services, Scientific Computing Theory and Data, Paul Scherrer Institute, CH-5232 Villigen PSI, Switzerland

*Correspondence to:
E-mail: roger.benoit@psi.ch

Abstract

The insertion of fusion proteins has enabled the crystallization of a wide range of G-protein-coupled receptors (GPCRs). Here, we explored the possibility of using a larger fusion protein, inserted into the third intracellular loop (ICL3) of β1-adrenoceptor (β1AR) via rigid chimeric helix fusions. The aim was to engineer a single-chain fusion protein that comprises sufficient mass and rigidity to allow single-particle cryo-EM data collection, without depending on binding proteins, such as G-proteins or nanobodies. Through parsing of the protein data bank (PDB), we identified the protein AmpC β-lactamase as a suitable candidate. Both termini of this protein are α-helical and the helices are antiparallel to each other. The distance between their centroids measures ~11 Å. Such a geometry is ideal to design extended chimeric helices with transmembrane (TM) helices 5 and 6 of β1AR, and the insertion of the protein adds ~39 kDa of mass to the receptor. We expressed the β1AR - AmpC β-lactamase fusion protein in mammalian cells. The binding of the antagonists propranolol and cyanopindolol to the purified fusion protein was confirmed by CPM-based thermofluor assays. The cryo-EM structure was solved to a nominal overall resolution of 3.6 Å and the seven helix architecture and helix eight were clearly resolved. Superimposition of the structure with known X-ray crystal structures of β1AR suggests that the protein is in its inactive conformation. The fusion protein described here provides a basis for high-throughput structure elucidation of class A GPCRs by cryo-EM for drug discovery research as well as for the elucidation of inactive state or wild-type GPCR structures. The fusion protein geometry theoretically fits a wide range of class A GPCRs and therefore can be applied to a multitude of receptors.

Introduction

Non-rhodopsin G-protein-coupled receptors (GPCRs) were for a long time among the most challenging protein drug targets for structural studies. The first structures of class A GPCRs were published in 2007 (Rasmussen et al., 2007) and in 2008 (Warne et al., 2008). Major bottlenecks for the structural biology studies of GPCRs include protein production, for example due to low expression levels or low protein stability, and crystallization, which can be challenging due to high conformational flexibility or a lack of hydrophilic surface area.

Two main strategies that revolutionized GPCR structural studies were the introduction of point mutations to improve the thermostability of the receptors (Warne et al., 2008), and the insertion of fusion proteins to stabilize a specific receptor conformation and/or to increase the soluble surface area for promoting the formation of ordered crystal contacts (Cherezov et al., 2007; Rosenbaum et al., 2007).

More recently, cryo-electron microscopy (cryo-EM) has emerged as a powerful alternative to X-ray crystallography and represents the next major progress in the field of GPCR structural biology. Protein structure elucidation at near-atomic resolution by single particle cryo-EM has seen an impressive increase in the number of structures published through the "resolution revolution", enabled by important technological advances in specimen preparation, as well as the development of direct electron detectors, and improvements in data analysis (Kühlbrandt, 2014).

The major advantage of using cryo-EM for structural studies is that only microgram quantities of protein are needed, and crystallization is not required. Nonetheless, due to their relatively small molecular mass (~45 kDa), combined with the relatively featureless shape within the detergent micelle, GPCRs remain challenging targets for single particles analysis, owing to the low signal-to-noise ratio and to the absence of prominent structural features that would be needed to achieve high accuracy in the determination of the angular orientation for 3D reconstructions (Nygaard et al., 2020).

In 2017, the first GPCR structures were solved by cryo-EM, both of them belonging to class B: the calcitonin receptor (CTR)(Liang et al., 2017) and the glucagon-like peptide-1 receptor (GLP-1)(Zhang et al., 2017). The structures of these receptors were solved in complex with the heterotrimeric G-proteins, along with the addition of a specific nanobody for stabilization purposes. The G-protein complex had a sufficient molecular mass for obtaining a good signal-to-noise ratio in single particle cryo-EM data collection and sufficiently clearly identifiable structural features for particle alignment. The complex formation relies on the binding of an agonist molecule that activates the receptor, therefore leading to the elucidation of active structures with G-protein or arrestin coupling (Huang et al., 2020; Staus et al., 2020; Zhang et al., 2021). To date, cryo-EM structures of GPCRs in their inactive conformation are therefore underrepresented.

Here, we solved the cryo-EM structure of a single-chain ß1AR - fusion protein in complex with the antagonist cyanopindolol. To the best of our knowledge, this is the first high-resolution GPCR cryo-EM structure that was solved in the absence of any artificial (e.g. nanobodies) or natural (e.g. G-proteins or arrestins) binding proteins. Because this protein does not require complex formation, the fusion protein approach we describe holds great promise as a tool for the elucidation of cryo-EM structures with different ligands at an increased throughput for drug discovery research.

Results and Discussion

Construct design

Our aim was to engineer a single-chain GPCR-fusion protein that contains sufficient mass and rigidity to allow cryo-EM structural studies at high resolution. Ultrastabilized β1-adrenergic receptor from *Meleagris gallopavo* (us-β1AR, pdb: 4BVN)(Miller-Gallacher et al., 2014) was our target of choice, because the expression and purification procedures for this protein were already well established in our lab. Furthermore, a high-resolution crystal structure of this β1AR construct was available, which enabled optimal validation of our cryo-EM results. While many fusion proteins that have been used in GPCR crystallography were connected to the receptor via loops and required stepwise optimization to achieve a certain degree of rigidity, some connections formed chimeric extended helices that are likely to be rigid also in solution, outside the crystal lattice (e.g. Wacker et al., 2017).

To identify a suited fusion protein that adds enough mass to the GPCR and that can be connected to the GPCR at ICL3 via such rigid, extended α-helices, structures in the PDB were filtered for the following criteria: 1) the protein chains are composed of more than 300 residues, 2) N- and C- termini are α-helical, 3) the terminal helices are approximately antiparallel to each other, and 4) terminal helices are close to 11 Å apart. These constraints were chosen to enable the scaffold protein to extend TM5 and TM6 in the ICL3 of class A GPCRs with minimal disruption.

Structures from the resulting list of hits were manually inspected, following additional selection criteria: 1) membrane proteins and oligomeric proteins were excluded, 2) proteins with available high-resolution structures were prioritized.

The AmpC β-lactamase (PDB entry 1FCO, Patera et al., 2000) from *E. coli* fulfilled all the desired criteria and we therefore used it for insertion into β1AR. The N- and C-terminal helices of β-lactamase were directly fused to the transmembrane helices TM5 and TM6 of β1AR.

Nine different constructs were designed in which 1) the transition between TM5 of the receptor and the N-terminus of the fusion protein and 2) the connection between the C-terminus of the fusion protein to TM6 of the receptor were optimized. The first construct, which we named construct 0/0, was designed based on visual inspection of the PDB structures of the receptor (PDB entry 2VT4, Warne et al. 2008) and of the fusion protein (PDB entry 1FCO, Patera et al. 2000). The remaining eight constructs were generated by adding or removing one codon at each of the receptor-fusion protein transitions.

The constructs, in a pcDNA 4/TO mammalian expression vector, included a C-terminal flexible linker comprising a human rhinovirus 3C protease (HRV 3C) cleavage site, followed by an eGFP for detection, and a twin strep tag for purification.

In addition to the nine us-β1AR constructs, the same construct design as for construct 0/0 was also applied to wild-type β1AR from *Meleagris gallopavo* (Uniprot: P07700), to test whether the β-lactamase fusion can sufficiently stabilize the receptor for expression and purification, without further stabilizing mutations.

Protein expression and purification

The GPCR fusion proteins were produced in stably transfected HEK293S Gnti- cells (Reeves et al. 2002). For expression tests, adherent cell cultures were used; for protein production, the cells were grown as suspension cultures.

To extract the protein of interest, membranes were solubilized using n-Dodecyl-β-D-Maltoside (β-DDM). Purification was performed by Strep-Tactin affinity chromatography followed by size-exclusion chromatography.
The purification of the proteins for cryo-EM analysis was performed in the presence of the high-affinity β1AR-binder cyanopindolol. The purification of proteins for biophysical characterization was performed in the absence of ligands. For cryo-EM analysis and for the biophysical characterization of the constructs, the C-terminal eGFP, which was fused to the protein of interest via a flexible linker, was removed by cleavage with HRV 3C protease (Figure 1).

Ligand-binding assays

CPM-based thermofluor assays were performed (not shown) on the three most diverse constructs, named -1/-1, 0/0 and +1/+1, to assess the stability and correct folding of the receptor in the fusion protein. The thermostability of the proteins was measured upon addition of increasing concentrations of cyanopindolol or propranolol, known antagonists for β1AR. The addition of the small molecule cyanopindolol resulted in a strong stabilizing effect on all tested constructs, while the addition of the small molecule propranolol had a less strong, but still significant stabilizing effect. Based on the thermostability data, construct 0/0 had the highest thermostability and was therefore chosen for cryo-EM specimen preparation.

Cryo-electron microscopy

After preliminary screening and optimization of the freezing conditions, the fusion protein particles were well distributed on the grids (Figure 2). For structure elucidation, we collected two datasets. As shown in Figure 2A, from the 2D classes, it was possible to visualize secondary structure elements, such as transmembrane helices of the receptor, as well as the fusion protein sticking out of the detergent micelle.
After motion correction and CTF estimation, a subset of movies were selected and particles were extracted and used for several cycles of 2D classification (Figure 2B). The best classes were selected for further processing steps (Figure 2C).
The size of the micelle was very large compared to the transmembrane receptor; therefore, its density was driving the alignment process in initial reconstruction attempts. To remove the signal of the micelle density, the reconstruction map was segmented to exclude the detergent density by carefully applying a soft mask around the detergent micelle (Figure 2D).
After segmentation, five different protein density signals were extracted as a trial-and-error approach to generate a soft mask around the region of interest for further refinements (Figure 2E). The highlighted volume (termed as trial #1) was chosen to perform 3D auto-refinement and focused classification to sort and remove the non-consensus particles (Figure 2F). To validate the signal subtraction procedures, the 2D classes of the protein regions and the 2D classes of the micelle regions were compared to assure that they did not contain major artefacts (Figure 2G). After validating the signal subtraction procedure, the particles corresponding to the four selected volumes after 3D sorting were re-centered and re-extracted to undergo non-uniform and local refinement, that resulted in a final map, with an overall resolution of 3.6 Å, with local resolutions ranging from 3.4 to 5.8 Å (Figure 2H).

Structure of the us-β1AR-β-lactamase fusion protein

Swiss-Modeler was used to generate a set of few initial models. Parts of these individual homology models were extracted and merged to produce an initial template for the subsequent modelling. The template model was rigid body fitted into the final cryo-EM map and this flexible fitted model was further mutated manually to fill the missing residues, alternating with real space refinement. The cryo-EM density allowed us to build 96% of the residue coverage of the expressed protein (Figure 2I).

Acknowledgments

We thank Mohamed Chami, Lubomir Kovacik and Carola Alampi at C-CINA Basel for support in cryo-EM data collection and the EM Facility at the PSI for technical support, and Takashi Ishikawa, Gebhard F.X. Schertler, Jan Pieter Abrahams, G.V. Shivashankar, Michel Steinmetz and Dmitry Veprintsev for supporting the project. We thank Hans Widmer, Sandra Jacob, Christian Wiesmann and Gregor Cicchetti for interesting discussions about the project. This work was supported by grants from Novartis FreeNovation, the Promedica Stiftung Chur (1401/M) and the Swiss National Science Foundation (SNF SPARK, CRSK-3_190414) to R.M.B..

Author contributions

The project was initiated and coordinated by R.M.B. The fusion proteins were designed by R.M.B.. The script for parsing the PDB was written by A.L. and S.B.. The protein was expressed by G.C. and T.B and purified by G.C.. Biophysical characterization was performed by G.C.. Grids for cryo-EM data collection were prepared and screened by G.C., I.M. and E.P.. Initial data analysis was performed by G.C. and E.P.. The cryo-EM structure was elucidated by G.C. and I.M.. The manuscript was written by G.C. and R.M.B. with contributions from all authors.

Competing interests

The authors declare no competing interests.

Materials and Methods

Fusion protein selection

Fusion proteins were identified using a Java program. BioJava (Lafita et al., 2019) was used for the analysis. All structures in the Protein Data Bank as of February 2017 were considered. Secondary structure was assigned using the DSSP algorithm (Kabsch and Sander, 1983), implemented in BioJava. Candidates were considered if they had 15 residues annotated as helical near both termini. The terminal helices were required to fall within 11±1Å apart, as measured at the helix centroid. Finally, helices were required to be antiparallel within 15°. Structures which matched the filter criteria were then manually inspected, with 1FCO chosen as the most promising candidate.
The source code and documentation to run the program can be found in the following open repository: https://github.com/lafita/motif-search

Transfection and stable cell line generation

HEK293 Gnti- cells were grown to ~90% confluence in a 100 mm diameter cell culture dish at 37°C, 5% CO_2. Transfection was performed using Lipofectamine 3000 reagent (Invitrogen) according to the standard protocol. 100 µg/ml Zeocin were used for stable cell line selection.

Protein expression

The stably transfected cells were first upscaled in adherent cultures and then transferred to suspension cultures. Suspension cultures were grown in PEM (Protein Expression Medium, Gibco) supplemented with 10% FBS, 1% GlutaMAX (GIBCO), Zeocin (Invivogen) to a final concentration of 100 µg/ml and Penicillin-Streptomycin (PAN Biotech) to a final concentration of 100 U/ml. The suspension cultures were grown in a shaker-incubator at 120 rpm, 37 °C, 5% CO_2. Cell densities were maintained between 800'000 and 1'500'000 cells/ml. Once the desired amount of cell culture volume was reached, the overexpression of the fusion protein was induced through the addition of tetracycline to a final concentration of 3 µg/ml. The induced cells were incubated for another 72 hours and then collected by centrifugation at 4'000 rpm, 15 min. at 4°C and stored at -80°C until further use.

Membrane preparation and protein solubilization

All subsequent steps were performed at 4 °C or on ice. The thawed cell pellets were resuspended in a pellet-to-buffer ratio of 1:5 in 50 mM HEPES, pH 7.5, 1 mM $MgCl_2$, 150 mM NaCl, supplemented with DNAse I and complete protease inhibitor cocktail (Roche). Cell membranes were disrupted using a dounce homogenizer. The homogenized material was ultracentrifuged at 230'000 rcf for 45 min., 4°C. The supernatant was discarded. The membranes were gently resuspended using an Ultra-turrax dispersing machine (IKA, USA) in solubilization buffer (50 mM HEPES, pH 7.5, 150 mM NaCl), supplemented with complete protease inhibitor cocktail (Roche). For solubilization, DDM was added to a final concentration of 1% (w/v). The mixtures were stirred at 150 rpm for 2 hours at 4 °C. Another ultracentrifugation step was used to clarify the solution containing the solubilized receptor.

Protein purification

The solubilized protein was incubated for 1 hour with washed and pre-equilibrated Strep-Tactin Superflow plus resin (Qiagen). The resin was then loaded into an Econo-Column Chromatography Column (Biorad) for gravity flow purification. The resin was washed 10 x with 2 volumes of wash buffer (50 mM HEPES, pH 7.5, 150 mM NaCl, 0.03 % (w/v) DDM). Stepwise protein elution was performed in wash buffer supplemented with 5 mM desthiobiotin (IBA-Lifesciences). The eluted protein was then treated with His-tagged human rhinovirus 3C protease (HRV 3C) to cleave off the C-terminal eGFP fusion and the tag. Reverse IMAC was performed to remove the protease. The protein was then concentrated to 0.5 ml using a 50 kDa cutoff concentrator (Vivaspin, Sartorius, MWCO 50 kDa).
Size-exclusion chromatography was carried out on a Superdex 200 increase 10/300 GL column (GE Healthcare) in 50 mM HEPES, pH 7.5, 100 mM NaCl, 0.03% (w/v) DDM, 1 µM cyanopindolol. The protein was concentrated to 3 mg/ml using a 50 kDa cutoff concentrator (Vivaspin, Sartorius). The purified protein was flash frozen in liquid nitrogen and stored at -80 ^{o}C.

Cryo-electron microscopy

Specimen preparation and data acquisition

For the final data collection, 3.5 µl of protein solution were applied onto the glow discharged Quantifoil Cu R1.2/1.3 200 grids (Electron Microscopy Sciences). The grids were blotted for 3s and plunge frozen into liquid ethane using a Vitrobot (Thermo Fisher Scientific), that was operated at 10 °C and 100% relative humidity. The grids were stored in liquid nitrogen for the high end data acquisition. Two datasets were collected in batches on a 300 KeV FEI Titan Krios transmission electron microscope with a GATAN post-column Quantum-LS energy filter (20 eV zero-loss filter). A total of 8600 movies were acquired in counting mode using SerialEM software package (Table 1). A total flux of 64 e-/Å^2 was used to record 40 dose fractionated frames. Initial preprocessing and pruning of the movies were analyzed in FOCUS during acquisition to filter the good micrographs.

Image processing and map reconstruction

The recorded movies were aligned and drift corrected using MotionCor2 (Zheng et al., 2017) by applying an appropriate dose weighting. The contrast transfer function (CTF) was estimated with either CTFFIND4 (Rohou and Grigorieff, 2015) or Gctf (Zhang, 2016) that resulted in excluding low-quality micrographs (based on CTF values above 7.0 Å and ice quality) from further image processing. The particles were auto-picked with Gautomatch (http://www.mrc-lmb.cam.ac.uk/kzhang) from the templates that were generated from the initial 2D classification job in CryoSPARC (Punjani et al., 2017). A total of 1.3 million particles were picked and subjected to three cycles of 2D classification to improve the SNR and image alignment. Both, Relion (v3.1) (Zivanov et al., 2018) and CryoSPARC (Punjani et al., 2017), were used in parallel for the processing and image alignments. After following the entire single particle pipeline, the reconstructed maps from CryoSPARC did not yield a better resolution map, although the 2D classes show clear indication of transmembrane (TM) secondary structural features. Thereafter, all the subsequent steps of image analysis were performed in the Relion 3.1 package. The selected good 2D classes (~520,000) were then used to perform three rounds of 3D classification in Relion with either K = 3, 4 or 6 classes. The 3D classification scheme with K=6 and tau=8 yielded a meaningful map comprising

295,000 particles (referred here to as good class), that was free of the junk and damaged protein particles. Further 3D auto refinement and CTF refinement iterations of this final set of particles did not improve the resolution, and the alignment was converged around 8.0 Å (FSC @ 0.143). All the above-described procedure was performed with three different box-sizes (256-, 320- and 360-pixels) and the 320-pixel extracted images yielded relatively better angular accuracies, and thus were selected for further processing.

Further improving the resolution and map quality involves signal subtracting of the detergent micelle density from the consensus 3D auto-refined map. To obtain a clear density for the seven transmembrane helices and the soluble domain, the map was segmented in Chimera (Pettersen et al., 2004) to generate different maps containing the protein-only signal. Then a soft mask was applied around the TM and soluble regions in order to extract the signal of interest from the protein-detergent micelle. The generously applied mask around the (trial #1) segmented region and subsequent signal subtraction yielded better results. Subsequent refinement and post-processing of the signal subtracted particles produced a better resolved map near 7 Å. To further improve the quality and resolution, the particles from this subtracted reconstruction were further sorted into 6 classes (without alignment and tau=12). The first four classes (highlighted) amounting to 165,000 particles were merged and the final map was reconstructed from the signal-subtracted 320-pixel sized images in CryoSPARC with a static mask around the region of interest. The final local refinement significantly improved the quality of the map to an overall resolution of 3.6 Å. The $FSC_{0.143}$ value from the CryoSPARC job yielded a relatively inflated value. The local resolution histogram plots show resolutions from 3.4 to 5.8 Å. Also, it was evident that the soluble domain was crucial in obtaining a high degree of the alignment accuracies, as the signal subtracted particles containing only the TM signal yielded a low quality map (data not shown).

To validate the signal subtraction procedure, the excluded micelle density was checked for accidental removal of the TM signal part. Local resolution maps were generated using Bsoft (Heymann, 2018) in CryoSPARC.

Model building

Swiss-Model (Waterhouse et al., 2018) was used to generate a set of few initial models from the reference PDB homologues (PDB entries 4BVN, 2BLS and 3GQZ). Parts of these individual homology models were extracted and merged to produce an initial template for the subsequent modelling. The template model was rigid body fitted into the final cryo-EM map in Chimera and later with MDFF (Trabuco et al., 2008) on the NAMD server. The flexible fitted model was further manually mutated to fill the missing residues in COOT (Emsley et al., 2010 and real space refinement in Phenix (Afonine et al., 2012) was performed. The cryo-EM density allowed to build 96% of the residue coverage of the expressed protein. The generated model was comprehensively validated and the overall statistics were improved by manually adjusting the clashed residues. The generated model was comprehensively validated as reported in Table 2.

References

Afonine, P. V., Grosse-Kunstleve, R. W., Echols, N., Headd, J. J., Moriarty, N. W., Mustyakimov, M., Terwilliger, T. C., Urzhumtsev, A., Zwart, P. H. & Adams, P. D. Towards automated crystallographic structure refinement with phenix.refine. Acta crystallographica. Section D, Biological crystallography 68, 352-367, doi:10.1107/s0907444912001308 (2012).

Cherezov V, Rosenbaum DM, Hanson MA, Rasmussen SG, Thian FS, Kobilka TS, Choi HJ, Kuhn P, Weis WI, Kobilka BK, Stevens RC. High-resolution crystal structure of an engineered human beta2-adrenergic G protein-coupled receptor. Science. 2007 Nov 23;318(5854):1258-65. doi: 10.1126/science.1150577. Epub 2007 Oct 25. PMID: 17962520; PMCID: PMC2583103.

Emsley P, Lohkamp B, Scott WG, Cowtan K. Features and development of Coot. Acta Crystallogr D Biol Crystallogr. 2010 Apr;66(Pt 4):486-501. doi: 10.1107/S0907444910007493. Epub 2010 Mar 24. PMID: 20383002; PMCID: PMC2852313.

Heymann, J. B. Guidelines for using Bsoft for high resolution reconstruction and validation of biomolecular structures from electron micrographs. Protein science: a publication of the Protein Society 27, 159-171, doi:10.1002/pro.3293 (2018).

Huang W, Masureel M, Qu Q, Janetzko J, Inoue A, Kato HE, Robertson MJ, Nguyen KC, Glenn JS, Skiniotis G, Kobilka BK. Structure of the neurotensin receptor 1 in complex with β-arrestin 1. Nature. 2020 Mar;579(7798):303-308. doi: 10.1038/s41586-020-1953-1. Epub 2020 Jan 16. PMID: 31945771; PMCID: PMC7100716.

Kabsch W, Sander C. Dictionary of protein secondary structure: pattern recognition of hydrogen-bonded and geometrical features. Biopolymers. 1983 Dec;22(12):2577-637. doi: 10.1002/bip.360221211. PMID: 6667333.

Kühlbrandt W. Biochemistry. The resolution revolution. Science. 2014 Mar 28;343(6178):1443-4. doi: 10.1126/science.1251652. PMID: 24675944.

Lafita A, Bliven S, Prlić A, Guzenko D, Rose PW, Bradley A, Pavan P, Myers-Turnbull D, Valasatava Y, Heuer M, Larson M, Burley SK, Duarte JM. BioJava 5: A community driven open-source bioinformatics library. PLoS Comput Biol. 2019 Feb 8;15(2):e1006791. doi: 10.1371/journal.pcbi.1006791. PMID: 30735498; PMCID: PMC6383946.

Liang YL, Khoshouei M, Radjainia M, Zhang Y, Glukhova A, Tarrasch J, Thal DM, Furness SGB, Christopoulos G, Coudrat T, Danev R, Baumeister W, Miller LJ, Christopoulos A, Kobilka BK, Wootten D, Skiniotis G, Sexton PM. Phase-plate cryo-EM structure of a class B GPCR-G-protein complex. Nature. 2017 Jun 1;546(7656):118-123. doi: 10.1038/nature22327. Epub 2017 Apr 24. PMID: 28437792; PMCID: PMC5832441.

Miller-Gallacher JL, Nehmé R, Warne T, Edwards PC, Schertler GF, Leslie AG, Tate CG. The 2.1 Å resolution structure of cyanopindolol-bound β1-adrenoceptor identifies an intramembrane Na+ ion that stabilises the ligand-free receptor. PLoS One. 2014 Mar 24;9(3):e92727. doi: 10.1371/journal.pone.0092727. PMID: 24663151; PMCID: PMC3963952.

Nygaard R, Kim J, Mancia F. Cryo-electron microscopy analysis of small membrane proteins. Curr Opin Struct Biol. 2020 Oct;64:26-33. doi: 10.1016/j.sbi.2020.05.009. Epub 2020 Jun 27. PMID: 32603877; PMCID: PMC7665978.

Patera, A.B., Blaszczak, L.C., Shoichet, B.K., 2000. Crystal structures of substrate and inhibitor complexes with AmpC beta-Lactamase: possible implications for substrateassisted catalysis. J. Am. Chem. Soc. 122, 10504–10512.

Pettersen, E. F., Goddard, T. D., Huang, C. C., Couch, G. S., Greenblatt, D. M., Meng, E. C. & Ferrin, T. E. UCSF Chimera--a visualization system for exploratory research and analysis. J Comput Chem 25, 1605-1612, doi:10.1002/jcc.20084 (2004).

Punjani, A., Rubinstein, J. L., Fleet, D. J. & Brubaker, M. A. cryoSPARC: algorithms for rapid unsupervised cryo-EM structure determination. Nature Methods 14, 290-296, doi:10.1038/nmeth.4169 (2017).

Rasmussen SG, Choi HJ, Rosenbaum DM, Kobilka TS, Thian FS, Edwards PC, Burghammer M, Ratnala VR, Sanishvili R, Fischetti RF, Schertler GF, Weis WI, Kobilka BK. Crystal structure of the human beta2 adrenergic G-protein-coupled receptor. Nature. 2007 Nov 15;450(7168):383-7. doi: 10.1038/nature06325. Epub 2007 Oct 21. PMID: 17952055.

Reeves PJ, Callewaert N, Contreras R, Khorana HG. Structure and function in rhodopsin: high-level expression of rhodopsin with restricted and homogeneous N-glycosylation by a tetracycline-inducible N-acetylglucosaminyltransferase I-negative HEK293S stable mammalian cell line. Proc Natl Acad Sci U S A. 2002 Oct 15;99(21):13419-24. doi: 10.1073/pnas.212519299. Epub 2002 Oct 7. PMID: 12370423; PMCID: PMC129688.

Rohou, A. & Grigorieff, N. CTFFIND4: Fast and accurate defocus estimation from electron micrographs. J Struct Biol 192, 216-221, doi:10.1016/j.jsb.2015.08.008 (2015).

Rosenbaum DM, Cherezov V, Hanson MA, Rasmussen SG, Thian FS, Kobilka TS, Choi HJ, Yao XJ, Weis WI, Stevens RC, Kobilka BK. GPCR engineering yields high-resolution structural insights into beta2-adrenergic receptor function. Science. 2007 Nov 23;318(5854):1266-73. doi: 10.1126/science.1150609. Epub 2007 Oct 25. PMID: 17962519.

Staus DP, Hu H, Robertson MJ, Kleinhenz ALW, Wingler LM, Capel WD, Latorraca NR, Lefkowitz RJ, Skiniotis G. Structure of the M2 muscarinic receptor-β-arrestin complex in a lipid nanodisc. Nature. 2020 Mar;579(7798):297-302. doi: 10.1038/s41586-020-1954-0. Epub 2020 Jan 16. PMID: 31945772; PMCID: PMC7367492.

Trabuco LG, Villa E, Mitra K, Frank J, Schulten K. Flexible fitting of atomic structures into electron microscopy maps using molecular dynamics. Structure. 2008 May;16(5):673-83. doi: 10.1016/j.str.2008.03.005. PMID: 18462672; PMCID: PMC2430731.

Wacker D, Wang S, McCorvy JD, Betz RM, Venkatakrishnan AJ, Levit A, Lansu K, Schools ZL, Che T, Nichols DE, Shoichet BK, Dror RO, Roth BL. Crystal Structure of an LSD-Bound Human Serotonin Receptor. Cell. 2017 Jan 26;168(3):377-389.e12. doi: 10.1016/j.cell.2016.12.033. PMID: 28129538; PMCID: PMC5289311.

Warne T, Serrano-Vega MJ, Baker JG, Moukhametzianov R, Edwards PC, Henderson R, Leslie AG, Tate CG, Schertler GF. Structure of a beta1-adrenergic G-protein-coupled receptor. Nature. 2008 Jul 24;454(7203):486-91. doi: 10.1038/nature07101. Epub 2008 Jun 25. PMID: 18594507; PMCID: PMC2923055.

Warne T, Edwards PC, Doré AS, Leslie AGW, Tate CG. Molecular basis for high-affinity agonist binding in GPCRs. Science. 2019 May 24;364(6442):775-778. doi: 10.1126/science.aau5595. Epub 2019 May 9. PMID: 31072904; PMCID: PMC6586556.

Waterhouse, A., Bertoni, M., Bienert, S., Studer, G., Tauriello, G., Gumienny, R., Heer, F. T., de Beer, T. A. P., Rempfer, C., Bordoli, L., Lepore, R. & Schwede, T. SWISS-MODEL: homology modelling of protein structures and complexes. Nucleic acids research 46, W296-w303, doi:10.1093/nar/gky427 (2018).

Zhang K. Gctf: Real-time CTF determination and correction. J Struct Biol. 2016 Jan;193(1):1-12. doi: 10.1016/j.jsb.2015.11.003. Epub 2015 Nov 19. PMID: 26592709; PMCID: PMC4711343.

Zhang Y, Sun B, Feng D, Hu H, Chu M, Qu Q, Tarrasch JT, Li S, Sun Kobilka T, Kobilka BK, Skiniotis G. Cryo-EM structure of the activated GLP-1 receptor in complex with a G protein. Nature. 2017 Jun 8;546(7657):248-253. doi: 10.1038/nature22394. Epub 2017 May 24. PMID: 28538729; PMCID: PMC5587415.

Zhang M, Gui M, Wang ZF, Gorgulla C, Yu JJ, Wu H, Sun ZJ, Klenk C, Merklinger L, Morstein L, Hagn F, Plückthun A, Brown A, Nasr ML, Wagner G. Cryo-EM structure of an activated GPCR-G protein complex in lipid nanodiscs. Nat Struct Mol Biol. 2021 Mar;28(3):258-267. doi: 10.1038/s41594-020-00554-6. Epub 2021 Feb 25. PMID: 33633398; PMCID: PMC8176890.

Zheng, S. Q., Palovcak, E., Armache, J. P., Verba, K. A., Cheng, Y. & Agard, D. A. MotionCor2: anisotropic correction of beam-induced motion for improved cryo-electron microscopy. Nat Methods 14, 331-332, doi:10.1038/nmeth.4193 (2017).

Zivanov, J., Nakane, T., Forsberg, B. O., Kimanius, D., Hagen, W. J., Lindahl, E. & Scheres, S.H. New tools for automated high-resolution cryo-EM structure determination in RELION-3. eLife 7, doi:10.7554/eLife.42166 (2018).

Figures

Figure 1) Biochemical analysis of the us-β1AR-AmpC β-lactamase 0/0 construct.

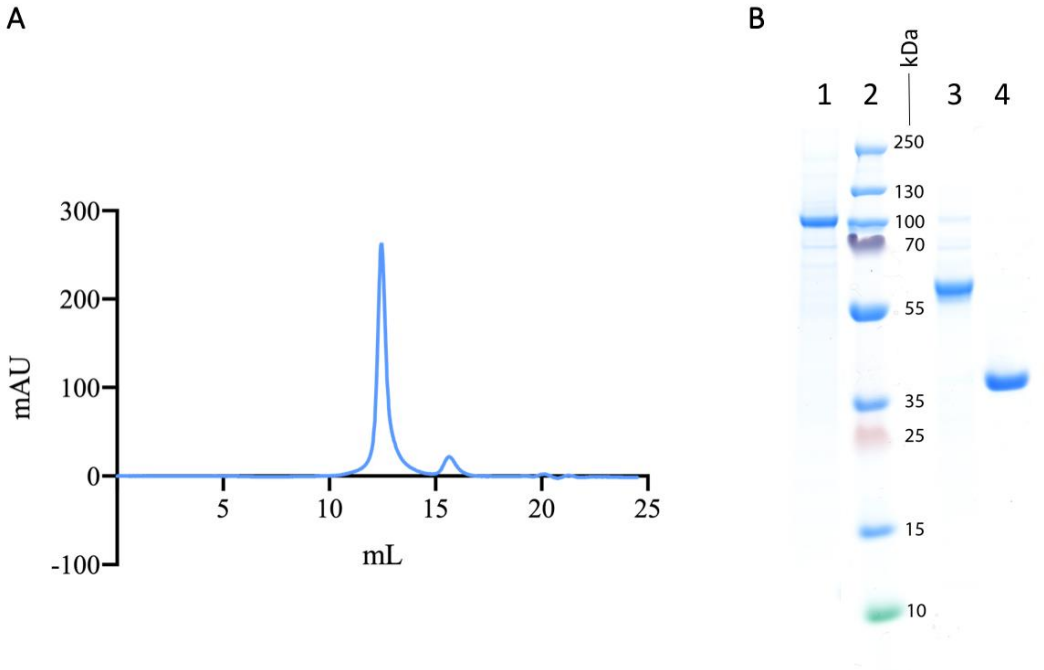

A) *Size-exclusion chromatogram (absorbance at 280 nm) of the cleaved fusion protein. The main peak corresponds to the us-β1AR-AmpC β-lactamase fusion protein, the smaller second peaks corresponds to the cleaved-off eGFP* ***B)*** *SDS-PAGE analysis of uncleaved and 3C HRV-cleaved us-β1AR-AmpC β-lactamase construct 0/0. 1) Uncleaved us-β1AR-AmpC β-lactamase with a C-terminal eGFP. 2) PageRuler Plus Prestained Protein Ladder (Thermo Scientific 26619). 3) HRV 3C cleaved us-β1AR-AmpC β-lactamase contruct 0/0. 4) Cleaved-off eGFP.*

Figure 2) Cryo-EM

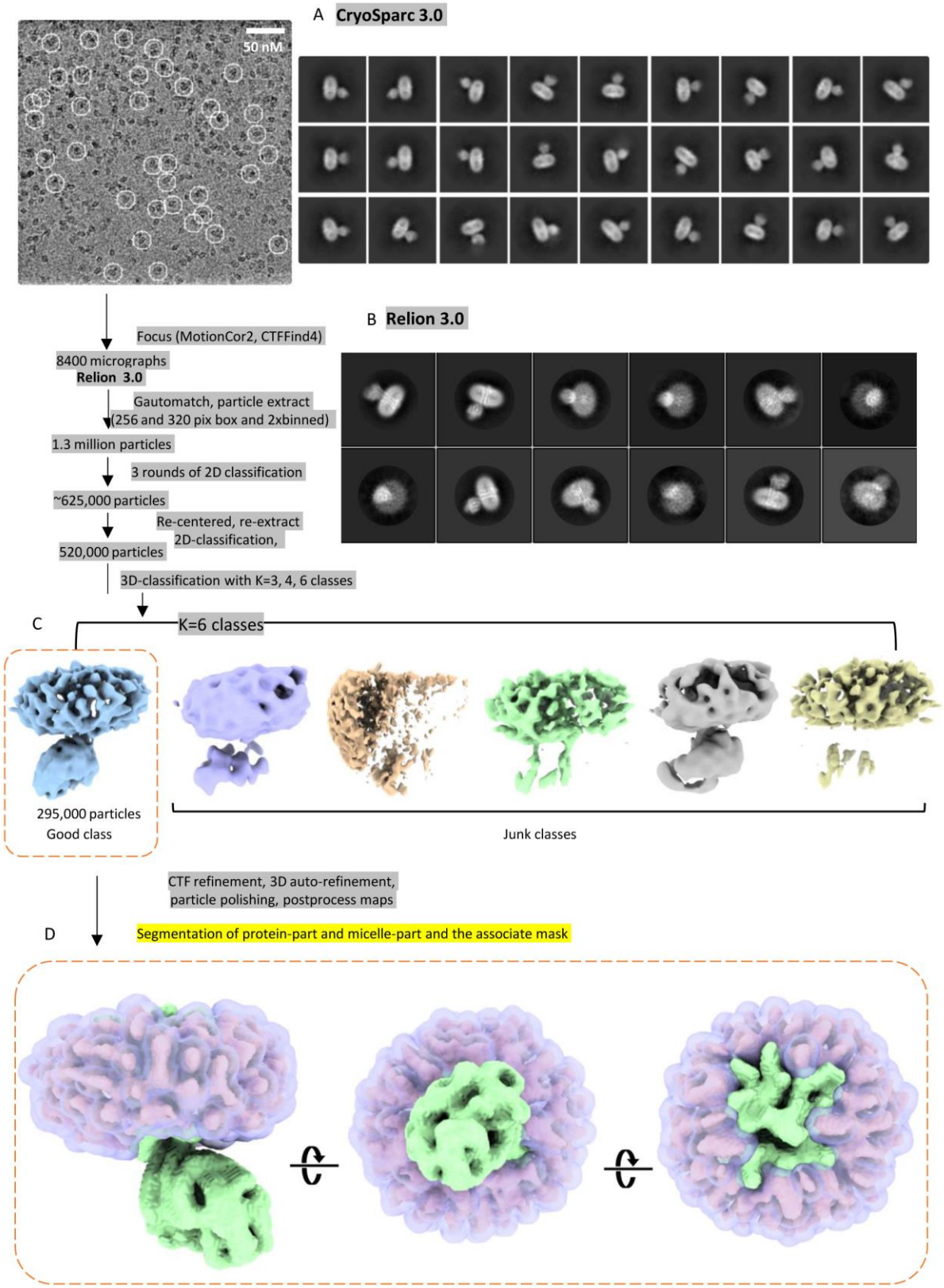

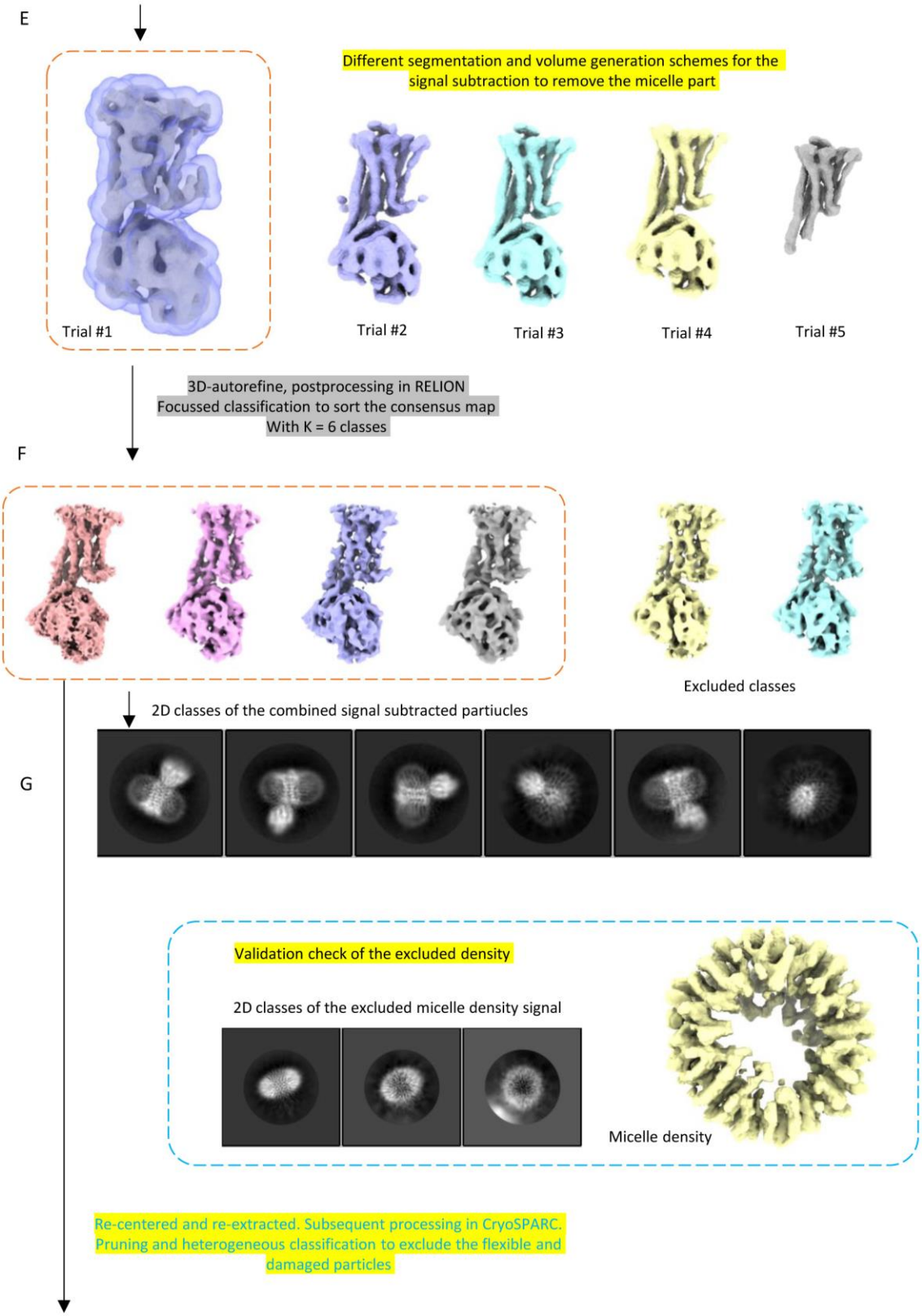
E
Different segmentation and volume generation schemes for the signal subtraction to remove the micelle part
Trial #1
Trial #2
Trial #3
Trial #4
Trial #5
3D-autorefine, postprocessing in RELION
Focussed classification to sort the consensus map
With K = 6 classes
F
Excluded classes
2D classes of the combined signal subtracted partiucles
G
Validation check of the excluded density
2D classes of the excluded micelle density signal
Micelle density
Re-centered and re-extracted. Subsequent processing in CryoSPARC.
Pruning and heterogeneous classification to exclude the flexible and damaged particles
Non-uniform and local refinement of the consensus map

H

Final map colored according to local resolution

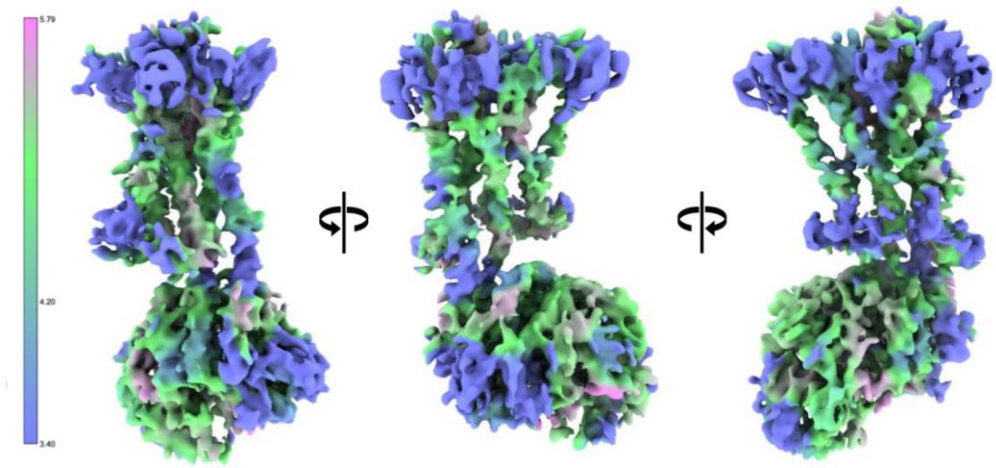

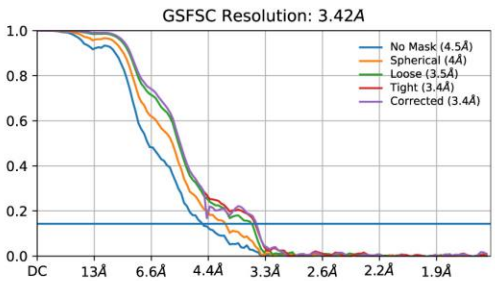

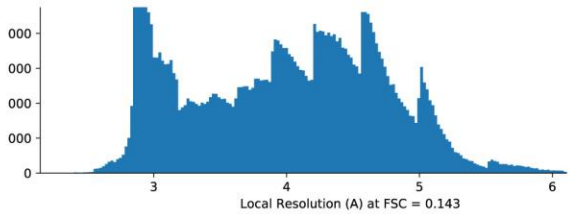

Local resolution histogram values

I

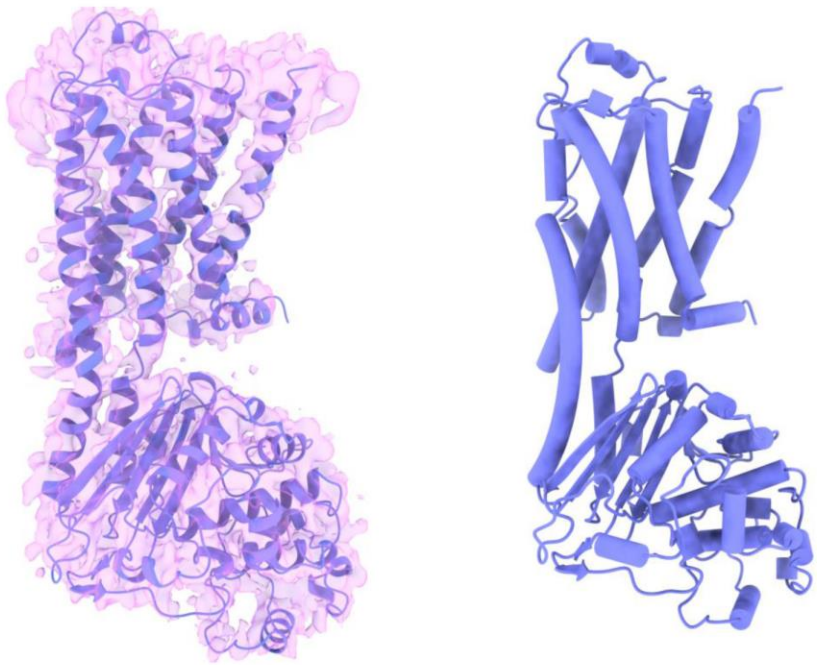

Tables

Table 1) Data acquisition parameters

Data acquisition parameters	**Dataset** **Protein: β1AR chimera**
Nominal magnification	165,000x
Camera and mode Pixel size	K2 (counting mode) 4k X 4k 0.82 Å
Total dose/movie # of frames # of movies	64 e-/Å2 40 8400
# of initial particles # of final particles (final map)	~ 520,000 ~ 165,000
Resolution : (FSC @ 0.143 criterion) unmasked masked	 4.5 Å 3.8 Å

Table 2) Validation and model statistics

Model	
Composition (#)	
Chains	1
Atoms	4957 (Hydrogens: 0)
Residues	Protein: 630 Nucleotide: 0
Water	0
Ligands	0
Bonds (RMSD)	
Length (Å) (# > 4σ)	0.003 (0)
Angles (°) (# > 4σ)	0.728 (1)
MolProbity score	1.66
Clash score	10.72
Ramachandran plot (%)	
Outliers	0.00
Allowed	2.55
Favored	97.45
Rama-Z (Ramachandran plot Z-score, RMSD)	
whole (N = 628)	1.16 (0.35)
helix (N = 313)	1.27 (0.30)
sheet (N = 42)	0.61 (0.77)
loop (N = 273)	0.36 (0.42)
Rotamer outliers (%)	0.00
Cβ outliers (%)	0.00
Peptide plane (%)	
Cis proline/general	5.7/0.0
Twisted proline/general	0.0/0.0
CaBLAM outliers (%)	1.60
ADP (B-factors)	
Iso/Aniso (#)	4957/0
min/max/mean	
Protein	58.45/321.67/163.08
Nucleotide	---
Ligand	---
Water	---
Occupancy	
Mean	1.00
occ = 1 (%)	100.00
0 < occ < 1 (%)	0.00
occ > 1 (%)	0.00
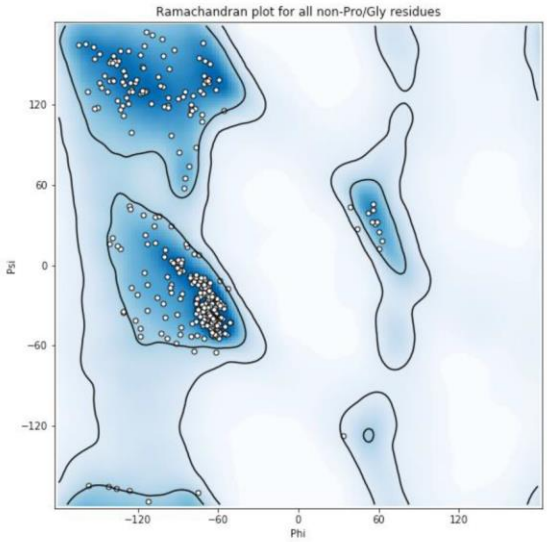
Model vs. Data	
CC (mask)	0.69
CC (box)	0.84
CC (peaks)	0.55
CC (volume)	0.68
Mean CC for ligands	---